35th Annual International Conference of the IEEE EMBS
Osaka, Japan, 3 - 7 July, 2013

Influence of the Anisotropic Mechanical Properties of the Skull in Low-Intensity Focused Ultrasound towards Neuromodulation of the Brain

Mohamed K. Metwally, Hee-Sok Han, Hyun Jae Jeon, Gon Khang, and Tae-Seong Kim, *Member, IEEE*

Abstract— **Lately, neuromodulation of the brain is considered one of the promising applications of ultrasound technology in which low-intensity focused ultrasound (LIFU) is used noninvasively to excite or inhibit neuronal activity. In LIFU, one of critical barriers in the propagation of ultrasound wave is the skull, which is known to be highly anisotropic mechanically: this affects the ultrasound focusing, thereby neuromodulation effects. This study aims to investigate the influence of the anisotropic properties of the skull on the LIFU via finite element head models incorporating the anisotropic properties of the skull. We have examined the pressure and stress distributions within the head in LIFU. Our results show that though most of the pressure that reaches to the brain is due to the longitudinal wave propagation through the skull, the normal stress in the transverse direction of the wave propagation has the main role to control the pressure profile inside the brain more than the shear stress. The results also show that the anisotropic properties of skull contribute in broadening the focal zone in comparison to that of the isotropic skull.**

I. Introduction

Ultrasound technology has a variety of applications in the medical field. Traditionally it has been used as a diagnostic imaging modality. Also it is utilized in high-intensity focused ultrasound (HIFU) for therapeutic applications like tumor-removal surgeries by noninvasively inducing heat to tissues, leading to irreversible tissue ablation. On the other side, it is possible to achieve reversible effects using low-intensity focused ultrasound (LIFU), which could be useful in neuromodulation to relieve the symptoms of depression, stroke, and Parkinson's disease as Fry predicted [1]. The studies have shown that neuromodulation, either excitation or inhibition, is possible using LIFU in the frequency range of 20-500 KHz [1], [2].

Although exploring LIFU started in parallel with HIFU, many aspects in LIFU remain unexplored. One of these aspects is investigating the parameters for energy delivery through the human skull where the skull is heterogeneous in terms of mechanical and acoustic properties.

There have been studies that have investigated the influence of the skull on HIFU or LIFU. Some HIFU studies used *in vivo* experiments to show the feasibility of delivering focused energy through the skull [3]. Many HIFU studies used analytically and *ex vivo* experiments to estimate the phase distortion to the propagating ultrasound waves that caused by the skull [4]. Few HIFU studies investigated the influence of skull inhomogeneity in terms of the sound speed and density on its focusing using finite difference method (FDM) [5]. Other HIFU studies used finite element method (FEM) to study the influence of the frequency and the scanning path on the focal zone and the resultant thermal effect, however a large portion of the skull was removed to avoid its distortion [6],[7].

Few LIFU studies investigated the ability of steering and focusing using a contact hemispherical ultrasound transducer without the skull-specific aberration correction [8], [9]. However, there is a lack of knowledge about the influence of the anisotropic mechanical properties of the skull on the pressure and stress distribution within the head.

In this paper, we have simulated LIFU using realistic finite element head models to examine the influence of the skull anisotropic properties on the pressure and stress distribution within the head. Two types of head models used in this study: a circular head model simplifying the effect of skull irregularity and thickness variance, and a realistic head model. First, LIFU was simulated with the circular head model with an application of a plane incident wave to get the basic understanding of the role of the anisotropic properties on the wave propagation within the head. Then the circular and realistic head models were used in LIFU simulations with the isotropic and anisotropic properties of the skull. Our results on the distribution of the pressure inside the skull during LIFU indicate that the normal stress in the transversal direction of the wave propagation has the main role on the propagation pattern inside the brain. Also the skull anisotropic properties broaden the focality on the degree of 19% and 13% in the longitudinal and the transverse directions respectively in the realistic head model.

II. Method

A. Generating 2-D FE Head Models

Two geometrical head shapes were considered as mentioned: the circular and realistic heads. The circular head was simulated to simplify the influence of the shape irregularity of the skull and the variations in the skull thickness which were considered in the realistic head model. The following four layers were considered: scalp, skull, cerebrospinal fluid (CSF), and brain. The models were simulated as immersed in water that has a radius of 18 cm.

1) Circular Head Model

The circular head model was simulated as four-concentric circles. The radius of scalp was 9 cm. The outer and inner radii of the skull were 8.4 cm and 7.6 cm respectively. The

Mohamed K. Metwally, Hee-Sok Han, Hyun Jae Jeon, Gon Khang, and Tae-Seong Kim are with the Department of Biomedical Engineering, Kyung Hee University, Yongin, Gyeonggi, Republic of Korea. (Corresponding author: +82-31-201-3731; fax: +82-31-201-3666; e-mail: tskim@ khu.ac.kr).

radius of brain was 7 cm. The thickness of the scalp and skull is in the range of literature [10-12].

2) Realistic Head Model

The realistic model was generated from a MR image slice acquired on a 3-T MRI scanner. The slice had dimensions of 212×181 with a voxel size of 1 mm^3. The brain was segmented using Freesurfer [13], while the scalp and skull regions were segmented using our in-house morphological techniques. Fig. 1 shows the two head models.

B. Isotropic and Anisotropic Properties

Two types of acoustical property settings were used in both models. The first one considered only the isotropic properties for all simulated layers, while the second considered the anisotropic properties of the skull. The CSF and brain were simulated as fluids because the values of density and sound speed in both are similar [14]. The isotropic properties of water were defined as the density ρ= 1000 kg/m^3 and the sound speed c = 1500 m/s [14]. The isotropic properties of the CSF were ρ= 1000 kg/m^3 [15] and c = 1508 m/s [16]. The isotropic properties of the brain were ρ= 1030 kg/m^3 [17] and c = 1550 m/s [14]. The isotropic mechanical properties of the scalp were ρ= 1100 kg/m^3 [19], the Young's modulus E = 16.7 MPa [20], and the Poisson's ratio ν= 0.42 [20]. The isotropic properties of the skull were ρ= 1413 kg/m^3 [8], the Young's modulus E = 5.2 GPa [22], and the Poisson's ratio ν= 0.22 [10]. For the anisotropic skull model, the Young's modulus in the radial direction (E_r) was 2.4 GPa and in the tangential direction (E_t) 5.6 GPa [23] with the shear modulus (G) was 3.5 GPa [24] and the Poisson's ratio ν= 0.22 [23].

C. Ultrasound Simulation

A circular transducer that has a length of 0.195 m and covers the range of angles of [-31π/180, 31π/180] symmetric around the negative x-axis was used instead of a linear transducer to generate 2 types of waves: plane and focused wave.

The plane wave was generated based on the following equation [24]:

$$\tau_i = \frac{|r|-|x_i|}{c} \quad (1)$$

where τ_i is the delay time of the i-th node on the circular transducer to generate the incident wave. x_i is the x-component of the i-th node on the circular transducer, r is the radius of the transducer, and c is the sound speed.

The focused wave was generated to achieve focusing at an arbitrary point on the x-axis within the brain based on the following equation [24]:

$$\tau_i = \frac{r_0-r_i}{c} \quad (2)$$

where r_0 is the distance between the central node on the circular transducer and the targeted focal point. r_i is the distance between the i-th node on the circular transducer and the targeted focal point. The simulated waves had a central frequency 70 KHz.

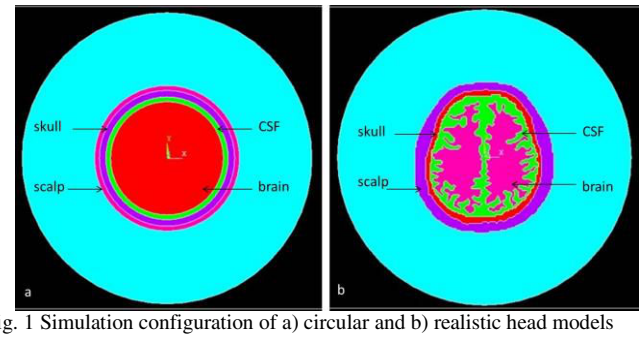

Fig. 1 Simulation configuration of a) circular and b) realistic head models

The pressure distribution within the fluid medium was computed by solving the second-order wave equation:

$$\left(\frac{\partial^2}{\partial x^2}+\frac{\partial^2}{\partial y^2}\right)p(x,y,t) = c^{-2}\frac{\partial^2 p(x,y,t)}{\partial t^2}. \quad (3)$$

The ultrasound propagation in fluid is converted into stress in the skull at the interface between the fluid and skull. The stress is derived from the particle displacement, based on the following equation [15]:

$$\frac{\partial p}{\partial n} = -\rho\frac{\partial^2 u_n}{\partial t^2} \quad (4)$$

where u_n is the displacement in the direction of the wave propagation. The sparse solver in ANSYS was used to calculate the pressure and stress distributions [25].

III. Results

The examined stress components include (i) shear stress, (ii) normal stress in the longitudinal direction (x-stress) which is the direction of wave propagation, and (iii) the normal stress in the transverse direction (y-stress) which is the normal direction to the wave propagation.

A. Plane Wave

Figs. 2 (a) and (b) show that the x-stress distribution within the skull is higher in the case of the isotropic skull than the anisotropic one. Figs. 2(c) and (d) show the distribution maps of the three types of stresses within the scalp and skull whose values survive the threshold of half of maximum of each stress. For example, the red region means that this area was affected by the x-stress, y-stress, and shear stress. However the value of the shear stress was the highest and exceeded the shear stress threshold value. This result indicates that the affected area by the y-stress and shear stress was enlarged in the case of the anisotropic model about 10% and 67% respectively as shown in Table 1.

B. Focused Wave

1) Circular Head Models

Figs. 3(a) and (b) show the influence of the skull anisotropic properties on the shape of the focal spot. The distribution maps of the stresses within the scalp and skull in Figs. 3(c) and (d) show that the affected area by the y-stress was translated from the lateral sides of the affected region in the isotropic model to the middle of this region in the anisotropic model.

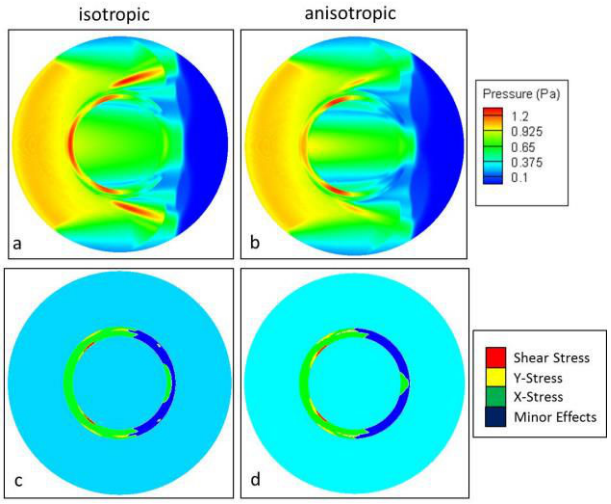

Fig. 2 Plane pressure distribution within the circular head model in the case of a) isotropic and b) anisotropic skull. Labeled maps of stresses within the scalp and skull in the case of c) isotropic and d) anisotropic skull properties.

To examine the effect of the anisotropic properties of the skull on focusing, three parameters were investigated: maximum pressure, focal length, and focal width. The focal length and width were defined to be the full width at a half of maximum of the focal spot within the brain region in the longitudinal and transverse directions respectively.

The skull anisotropy reduced the maximum pressure within the focal spot slightly about 9%, and expanded the focal length and width about 7% and 9% respectively as shown in Table 2.

2) Realistic Head Models

In the realistic head model, the wave got focused while considering the isotropic and anisotropic skull. Figs. 4 (a) and (b) show the longitudinal stress distribution within the scalp and skull while Figs. 4(c) and (d) show the stresses distribution maps.

Note that the focality was reduced with the skull anisotropy where the focal length was expanded about 19% and the focal width about 13% while the maximum pressure was damped slightly about 5% as shown in Table 2.

IV. Discussion

A. Plane Wave

The plane wave study using the circular head model was conducted to understand the interaction between the propagated wave and the skull anisotropic properties. The results show that the x-stress within the skull is proportional to the Young's modulus. Therefore, the x-stress in the anisotropic model is low in the regions where the radial component of the Young's modulus is directed longitudinally

Table 1 The affected skull regions by stresses in the case of plane wave

Model Type	X-Stress (cm^2)	Y-Stress (cm^2)	Shear Stress (cm^2)
Isotropic	45	4.93	1.24
Anisotropic	39	5.42	2

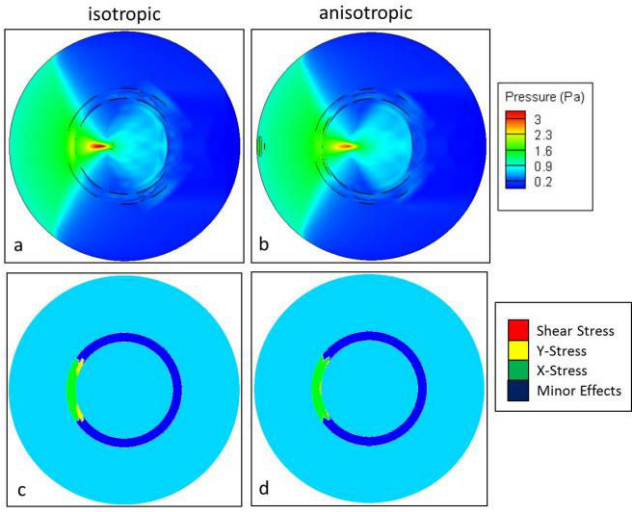

Fig. 3 Focused pressure distribution within the circular head model in the case of a) isotropic and b) anisotropic skull. Labeled maps of stresses within the scalp and skull in the case of c) isotropic and d) anisotropic skull properties

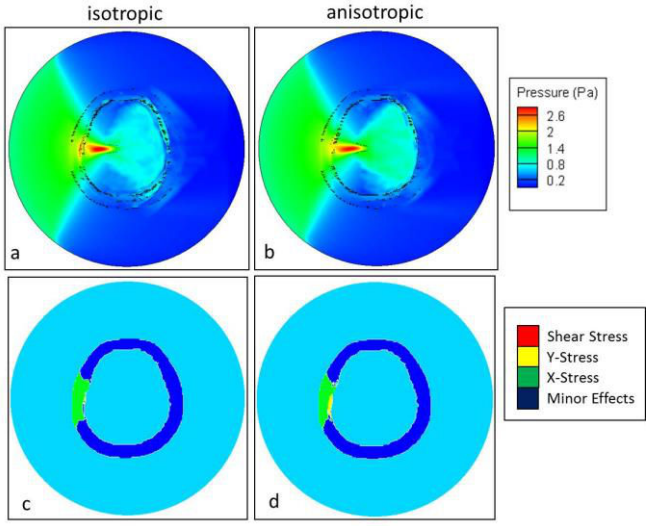

Fig. 4 Focused pressure distribution within the realistic head model in the case of a) isotropic and b) anisotropic skull. Labeled maps of stresses within the scalp and skull in the case of c) isotropic and d) anisotropic skull properties.

Table 2 Quantitative analysis of the focal spot in the circular and realistic head models with respect to the properties of the skull

Model Type		Focal Spot		
		Max. Pressure (Pa)	*Focal Length (cm)*	*Focal Width (cm)*
Circular Head Model	Isotropic	3.11	2.73	1.40
	Anisotropic	2.82	2.91	1.52
Realistic Head Model	Isotropic	2.82	2.12	1.45
	Anisotropic	2.68	2.53	1.64

and lower than that of x-stress in the isotropic model, while the tangential Young's modulus in the same direction resulting in higher values of the x-stress.

On the other hand, the tangential Young's modulus and the shear modulus dissipate the incident energy in the forms of y-stress and shear stress. This effect occurs when these modulus are almost in the longitudinal direction with respect to the incident wave. The locations and the area of the affected regions by the y-stress affect the pressure profile inside the brain. These areas in the anisotropic model are wider than that in the isotropic, resulting in narrowing the skull region that the incident wave passes through, leading to more a concise propagation pattern inside the brain

B. Focused Wave

The skull anisotropy affects the focality by damping the maximum pressure in the focal spot and expanding its dimension. These effects take place because of generating the affected region by the y-stress within the path of the propagated wave, where energy dissipation occurs, leading to some phase distortion.

V. CONCLUSION

This study aimed at investigating the influence of the anisotropic properties of the skull on LIFU. The pressure and stress distributions within the head were examined by utilizing the realistic finite element head models incorporating the isotropic and anisotropic properties of the skull. The results indicate that the normal stress in the transverse direction to the wave propagation direction within the skull is the main factor that forms the pressure profile inside the brain. The anisotropic properties tend to decrease the focal pressure and expand the size of the focal spot about 19% and 13% in the longitudinal and the transverse directions respectively in the realistic head model. Towards neuromodulation using LIFU, one needs to consider the skull anisotropy and adjust the parameters accordingly.

ACKNOWLEDGMENTS

This work was supported by the National Research Foundation of Korea (NRF) grant funded by the Korea government (MEST) (2011-0029485).

REFERENCES

[1] A. Bystritsky , A. S. Korb, P. K. Douglas, M. S. Cohen, W. P. Melega, A. P. Mulgaonkar, A. DeSalles, B. –K. Min, S. –S. Yoo," A review of low-intensity focused ultrasound pulsation". Brain Stimulation, vol. 4, issue 3, pp. 125-136, 2011.

[2] F. Ahmadi, I. V. McLoughlin, S. Chauhan, G. ter-Haar," Bio-effects and safety of low-intensity, low-frequency ultrasonic exposure". Progress in biophysics and molecular biology, vol. 108, Issue 3, pp. 119-138, 2012.

[3] K . Hynynen, F.A. Jolesz," Demonstration of potential noninvasive ultrasound brain therapy through an intact skull". Ultrasound in Medicine & Biology, vol. 24, Issue 2, pp. 275–283, 1998.

[4] G. T. Clement, K. Hynynen," Correlation of ultrasound phase with physical skull properties". Ultrasound in Medicine & Biology, vol. 28, Issue 5, pp. 617–624, 2002.

[5] G. Pinton, J. –F. Aubry, M. Fink, M. Tanter," Effects of nonlinear ultrasound propagation on high intensity brain therapy". IEEE international ultrasonics symposium proceedings, 2009.

[6] S. Behnia, A. Jafari, F. Ghalichi, A. Bonabi," Finite-element simulation of ultrasound brain surgery: effects of frequency, focal pressure, and scanning path in bone heating reduction". Central European Journal of Physics, vol. 6, issue 2, pp. 211-222, 2008.

[7] F. Sharifi, H. Ahmadikia, S. Amohammadi," Three dimensional modeling of high intensity focused ultrasound brain tumor treatment using finite element simulation method". ICBME proceedings, 2010.

[8] X. Yin, K. Hynynen," A numerical study of transcranial focused beam propagation at low frequency". Physics in medicine and biology, vol. 50, pp. 1821-1836, 2005.

[9] F.-Y. Yang, T.-J. Mao, Y.-Y. Chen, H. Chang, W.-L. Lin," Beam steering and focusing ability of a contact ultrasound transducer for transskull brain disease therapy". Biomedical Engineering – Applications, Basis and Communications, vol. 18, issue 6, pp. 328-336, 2006.

[10] T. L. Skytte, " Forensic Finite Element Simulation of Skull Fracture". Riso DTU, National Laboratory of Sustainable Energy, 2010.

[11] A. J. Lupin, R. J. Gardiner," Scalp thickness in the temporal region: its relevance to the development of cochlear implants". Cochlear Implants International, pp.30–38, 2001.

[12] S. Kleiven," Finite Element Modeling of the Human Head". PhD thesis, Royal Institute of Technology, 2002.

[13] http://surfer.nmr.mgh.harvard.edu/

[14] Y. Liu," Wave Propagation Study Using Finite Element Analysis". M.S. thesis, university of Illinois at urbana-Champaign,2002.

[15] S.-H. Kim, H. S. Suh, M. H. Cho, S. Y. Lee, T.-S. Kim," Finite Element Simulation of Ultrasound Propagation in Bone for Quantitative Ultrasound toward the Diagnosis of Osteoporosis". Conference Proceeding IEEE EMBS 2009.

[16] E. Levin, S. Muravchick, and M. I. Gold," Density of Normal Human cerebrospinal fluid and Tetracaine Solutions", Journal of Anesthesia and Analgesia, vol. 60, No. 11, pp. 814-817, 1981.

[17] L. Palaniappan, V. Velusamy," Ultrasonic study of human cerebrospinal fluid", Indian journal of pure and applied physics, vol. 42, pp. 591-594, 2004.

[18] D. A. Chrostensen, " Ultrasonic Bioinstrumentation". USA, CA: John Wiley & Sons,1988.

[19] A. Kiourti, K. S. Nikita," Numerical Assessment of the Performance of a Scalp-Implantable Antenna: Effects of Head Anatomy and Dielectric Parameters". Bioelectromagnetics, 2012.

[20] T. J. Horgan, M. D. Gilchrist," The Creation of Three-Dimensional Finite Element Models for Simulating Head Impact Biomechanics". International Journal of Crashworthiness, vol.8. ISN. 4, pp.353-66, 2003.

[21] R. Delillea, D. Lesueura, P. Potierb, P. Drazetica, E. Markiewicza, " Experimental study of the bone behavior of the human skull bone for the development of a physical head model". International Journal of Crashworthiness, vol. 12 No. 2 pp. 101–108, 2007.

[22] J. H. Mcelhaney, J. L. Fogle. J. W. Melvin, R. R. Haynes, V. L. Roberts, N. M. Alem, " Mechanical properties of cranial bone". Journal of Biomechanics, vol. 3.p. 495-511. 1970.

[23] http://www.engin.umich.edu/class/bme456/bonefunction/bonefunction.htm

[24] J. L. Prince, J. M. Links," Medical Imaging Signals and Systems". USA, Pearson Prentice Hall. 2006.

[25] ANSYS available: http://www.ansys.com